Development and integration of xerogel polymeric absorbance micro-filters into lab-on-chip systems

Ester Carregal-Romero,[1,2] César Fernández-Sánchez,[1,5] Alma Eguizabal,[3] Stefanie Demming,[4] Stephanus Büttgenbach,[4] and Andreu Llobera[1,*]

[1]*Instituto de Microelectrónica de Barcelona IMB-CNM (CSIC), Campus UAB, 08193, Bellaterra, Barcelona, Spain*
[2]*Estudis de Doctorat Ciència de Materials, Universitat Autònoma de Barcelona, 08193, Bellaterra, Spain*
[3]*Grupo de Ingeniería Fotónica, Universidad de Cantabria, 39005, Santander, Spain*
[4]*Institut für Mikrotechnik, Technische Universität Braunschweig, Braunschweig, 38106, Germany*
[5]*cesar.fernandez@imb-cnm.csic.es*
[*]*andreu.llobera@imb-cnm.csic.es*

Abstract: This work reports on the implementation of different absorption micro-filters based on a dye-doped hybrid organic-inorganic xerogel polymeric material synthesized by the sol-gel process. Microstructures containing eight different filter widths were fabricated in polydimethylsiloxane (PDMS), bonded to glass substrates and filled with the corresponding dye doped polymeric material by a soft lithography approach. The filtering capacity as a function of dye concentration and filter width was studied and revealed a linear dependence with both parameters, as expected according to the Beer-Lambert law. Zero passband transmittance values and relatively sharp stopband regions were achieved with all the filters, also showing rejection levels between −6 dB and −55 dB. Finally, such filters were monolithically integrated into a disposable fluorescence-based photonic lab-on-a-chip (PhLoC) approach. Calibration curves carried out with a model fluorophore target analyte showed an over two-fold increase in sensitivity and a thirty-fold decrease of the limit of detection (LOD) compared with the values recorded using the same PhLoC system but without the polymeric filter structure. The results presented herein clearly indicate the feasibility of these xerogel-based absorbance filtering structures for being applied as low-cost optical components that can be easily incorporated into disposable fluorescence-based photonic lab on a chip systems.

OCIS codes: (130.0130) Integrated optics; (230.7408) Wavelength filtering devices; (350.2450) Filters, absorption; (160.0160) Materials; (160.6060) Solgel.

References and links

1. S. M. Borisov and O. S. Wolfbeis, "Optical biosensors," Chem. Rev. **108**(2), 423–461 (2008).
2. M. Dandin, P. Abshire, and E. Smela, "Optical filtering technologies for integrated fluorescence sensors," Lab Chip **7**(8), 955–977 (2007).
3. H. A. Macleod, "Thin Film Optical Filters" (Institute of Physics Publishing, London, 2001)
4. M. L. Chabinyc, D. T. Chiu, J. C. McDonald, A. D. Stroock, J. F. Christian, A. M. Karger, and G. M. Whitesides, "An integrated fluorescence detection system in poly(dimethylsiloxane) for microfluidic applications," Anal. Chem. **73**(18), 4491–4498 (2001).
5. A. H. Mahan, R. Biswas, L. M. Gedvilas, D. L. Williamson, and B. C. Pan, "On the influence of short and medium range order on the material band gap in hydrogenated amorphous silicon," J. Appl. Phys. **96**(7), 3818–3826 (2004).
6. O. Hofmann, X. Wang, A. Cornwell, S. Beecher, A. Raja, D. D. Bradley, A. J. Demello, and J. C. Demello, "Monolithically integrated dye-doped PDMS long-pass filters for disposable on-chip fluorescence detection," Lab Chip **6**(8), 981–987 (2006).

#168632 - $15.00 USD Received 15 May 2012; revised 6 Jul 2012; accepted 23 Jul 2012; published 1 Oct 2012

7. A. Llobera, S. Demming, H. N. Joensson, J. Vila-Planas, H. Andersson-Svahn, and S. Büttgenbach, "Monolithic PDMS passband filters for fluorescence detection," Lab Chip **10**(15), 1987–1992 (2010).
8. M. Yamazaki, O. Hofmann, G. Ryu, L. Xiaoe, T. K. Lee, A. J. deMello, and J. C. deMello, "Non-emissive colour filters for fluorescence detection," Lab Chip **11**(7), 1228–1233 (2011).
9. C. Richard, A. Renaudin, V. Aimez, and P. G. Charette, "An integrated hybrid interference and absorption filter for fluorescence detection in lab-on-a-chip devices," Lab Chip **9**(10), 1371–1376 (2009).
10. L. L. Hench and J. K. West, "The sol-gel process," Chem. Rev. **90**(1), 33–72 (1990).
11. J. Y. Wen and G. L. Wilkes, "Organic/inorganic hybrid network materials by the sol-gel approach," Chem. Mater. **8**(8), 1667–1681 (1996).
12. C. Sanchez and F. Ribot, "Design of hybrid organic-inorganic materials synthesized via sol-gel chemistry," New J. Chem. **18**, 1007–1047 (1994).
13. B. Lebeau and P. Innocenzi, "Hybrid materials for optics and photonics," Chem. Soc. Rev. **40**(2), 886–906 (2011).
14. A. Llobera, V. J. Cadarso, E. Carregal-Romero, J. Brugger, C. Domínguez, and C. Fernández-Sánchez, "Fluorophore-doped xerogelantiresonant reflecting optical waveguides," Opt. Express **19**(6), 5026–5039 (2011).
15. N. Tohge, M. Hasegawa, N. Noma, K. Kintaka, and J. Nishii, "Fabrication of two-dimensional gratings using photosensitive gel films and their characterization," J. Sol-Gel Sci. Technol. **26**(1/3), 903–907 (2003).
16. X. H. Zhang, W. Que, C. Y. Jia, J. X. Hu, and W. G. Liu, "Fabrication of micro-lens arrays built in photosensitive hybrid films by UV-cured imprinting technique," J. Sol-Gel Sci. Technol. **60**(1), 71–80 (2011).
17. C. Fernández-Sánchez, V. J. Cadarso, M. Darder, C. Dominguez, and A. Llobera, "Patterning high-aspect-ratio sol-gel structures by microtransfer molding," Chem. Mater. **20**(8), 2662–2668 (2008).
18. C. Sanchez, P. Belleville, M. Popall, and L. Nicole, "Applications of advanced hybrid organic-inorganic nanomaterials: from laboratory to market," Chem. Soc. Rev. **40**(2), 696–753 (2011).
19. Y. N. Xia and G. M. Whitesides, "Soft lithography," Angew. Chem. Int. Ed. **37**(5), 550–575 (1998).
20. D. Avnir, D. Levy, and R. Reisfeld, "The nature of the silica cage as reflected by spectral changes and enhanced photostability of trapped Rhodamine-6G," J. Phys. Chem. **88**(24), 5956–5959 (1984).
21. G. Schottner, "Hybrid sol-gel-derived polymers: Applications of multifunctional materials," Chem. Mater. **13**(10), 3422–3435 (2001).
22. M. Zayat, R. Pardo, E. Castellón, L. Torres, D. Almendro, P. G. Parejo, A. Álvarez, T. Belenguer, S. García-Revilla, R. Balda, J. Fernández, and D. Levy, "Optical and Electro-optical Materials Prepared by the Sol-Gel Method," Adv. Mater. (Deerfield Beach Fla.) **23**(44), 5318–5323 (2011).
23. P. Escribano, B. Julian-Lopez, J. Planelles-Arago, E. Cordoncillo, B. Viana, and C. Sanchez, "Photonic and anobiophotonic properties of luminescent lanthanide-doped hybrid organic-inorganic materials," J. Mater. Chem. **18**(1), 23–40 (2007).
24. R. Pardo, M. Zayat, and D. Levy, "Photochromic organic-inorganic hybrid materials," Chem. Soc. Rev. **40**(2), 672–687 (2011).
25. A. Llobera, R. Wilke, and S. Büttgenbach, "Poly(dimethylsiloxane) hollow Abbe prism with microlenses for detection based on absorption and refractive index shift," Lab Chip **4**(1), 24–27 (2004).
26. A. Llobera, S. Demming, R. Wilke, and S. Büttgenbach, "Multiple internal reflection poly(dimethylsiloxane) systems for optical sensing," Lab Chip **7**(11), 1560–1566 (2007).
27. B. H. Jo, L. M. Van Lerberghe, K. M. Motsegood, and D. J. Beebe, "Three-dimensional micro-channel fabrication in polydimethylsiloxane (PDMS) elastomer," J. Microelectromech. Syst. **9**(1), 76–81 (2000).
28. R. Ulrich and R. Torge, "Measurement of thin film parameters with a prism coupler," Appl. Opt. **12**(12), 2901–2908 (1973).
29. R. H. Glaser, G. L. Wilkes, and C. E. Bronnimann, "Solid-state ^{29}Si NMR of TEOS-based multifunctional sol-gel materials," J. Non-Cryst. Solids **113**(1), 73–87 (1989).
30. P. Lacan, C. Guizard, and L. Cot, "Chemical and rheological investigations of the sol-gel transition in organically-modified siloxanes," J. Sol-Gel Sci. Technol. **4**(2), 151–162 (1995).
31. A. Llobera, R. Wilke, and S. Büttgenbach, "Optimization of poly(dimethylsiloxane) hollow prisms for optical sensing," Lab Chip **5**(5), 506–511 (2005).
32. V. Thomsen, D. Shatzlein, and D. Mercuro, "Limits of Detection in Spectroscopy," Spectroscopy **18**, 112–114 (2003).
33. A. Pais, A. Banerjee, D. Klotzkin, and I. Papautsky, "High-sensitivity, disposable lab-on-a-chip with thin-film organic electronics for fluorescence detection," Lab Chip **8**(5), 794–800 (2008).
34. B. Yao, G. Luo, L. Wang, Y. Gao, G. Lei, K. Ren, L. Chen, Y. Wang, Y. Hu, and Y. Qiu, "A microfluidic device using a green organic light emitting diode as an integrated excitation source," Lab Chip **5**(10), 1041–1047 (2005).

1. Introduction

One of the most common approaches in photonic lab-on-a-chip (PhLoC) systems is the measurementof fluorescence as detection method [1]. Optical filtering is often required to be implemented in these systems due to the following main reasons. In fluorescence spectroscopy the intensity of the excitation light is typically orders of magnitude larger than

#168632 - $15.00 USD Received 15 May 2012; revised 6 Jul 2012; accepted 23 Jul 2012; published 1 Oct 2012

the fluorescence light of the fluorophore target molecule. Additionally, the Stokes shift of fluorophore molecules is usually very small, which makes it even more difficult to discriminate between the excitation and emission signals. The more accepted filtering configurations suitable to perform such discrimination are based on interferometric and absorbance-based approaches [2]. Interferometric filters consist in alternating layers of high- and low-refractive-index materials. In spite of these filters showing high absorbance levels at the stopband with sharp bands and zero passband penalties they suffer from serious drawbacks. First, the absorption depends on the angle of the incidence light [3]. Second, the thickness of the layers has to be perfectly controlled in order to obtain filtering at the required wavelength, which makes the fabrication an expensive and critical process. These effects hamper its integration into PhLoC. Conversely, absorbance filters are generally fabricated with a single layer of a material containing a chromophore [4] or a band gap material [5]. In both cases, they are fabricated to show high absorption at the excitation wavelength and low absorption at the fluorescence wavelength of the solution or compound being measured. The performance of such absorbance filters is governed by the Beer-Lambert law and, unlike interferometric filters, their response is independent of the beam incidence angle [2].

Because of their simplicity, robustness and low cost, absorbance filters are more suitable for being integrated into disposable PhLoCs, although their optical properties are more limited when compared with their interferometric counterparts. The material synthesis and fabrication processes can also be designed to be simple and not time-consuming. Several attempts have been previously reported for this configuration. Hoffman *et. al.* [6] used a millimeter-thick dye-doped PDMS film as a fluorescence filter. In order to get an adequate dispersion of the dye in the polymer matrix they use toluene, a toxic solvent that has to be completely removed if the system is being used for bio-applications. In a previous work, we overcome this problem [7] by fabricating PDMS-based filters of varying width using red, green and blue ink directly mixed with the PDMS pre-polymer solution. However, the resulting filters exhibited broad stop band values (ranging from 100 to 150 nm) and non-zero passband values, which limit their applicability. Yamazaki *et. al.* [8] reported colored filters based on a porous titanium oxide film onto which a monolayer of dye molecules was defined. The fabrication involves the sintering of a titania film at 450° C, which limits their compatibility with polymeric substrates and/or low temperature fabrication methods, making difficult the implementation of these filters into low-cost microsystems. Richard *et. al.* [9] presented an integrated hybrid absorption and interference filter based on a dye doped epoxy-based photoresist, obtaining with the absorption layers high rejection levels at the stopband with narrow optical path lengths(0.8-2 μm). Nevertheless, these filters can only act like high-pass filters (passband @ 650 nm) with broad stopband widths (> 250 nm) limiting their applicability in fluorescence detection since most common analytes show emission wavelengths below this value. Moreover, at the optimized maximum dye concentration they did not succeed in developing patterns (e.g. channels), and also the photoresist solvents make this approach not biocompatible.

An alternative absorbance filtering approach that circumvents the drawbacks of those above-mentioned absorbance filter approaches is described in this work. Dye-doped organic-inorganic silicate-based glasses fabricated by sol-gel technology from aqueous solutions were applied to the patterning of absorbance micro-filters by soft lithography, which could be easily implemented in PhLoCs.The sol-gel process consists in the formation of a polymeric network by the hydrolysis and polycondensation of metallic alcoxides [10]. The most widely used precursors in sol-gel technology are silane-derived monomers such as tetramethylorthosilicate (TMOS) and tetraethyl orthosilicate (TEOS). Working with these molecules, silanol groups (≡Si-OH) are generated by hydrolysis reactions in hydroalcoholic solutions usually containing an acid or basic catalyst. Polycondensation reactions involving these groups give riseto siloxane bonds (≡Si-O-Si≡). A polysiloxane network is thus formed and alcohol and water are generated as sub-products. This network is next cured and dried to

#168632 - $15.00 USD Received 15 May 2012; revised 6 Jul 2012; accepted 23 Jul 2012; published 1 Oct 2012

eventually give rise to a xerogel polymer structure. Indeed, if the hydrolysis and condensation reactions with the above mentioned monomers take place with a 100% yield, a silicon oxide network is obtained. A family of sol-gel like materials that show promising properties is that formed by the so-called organic-inorganic hybrid polymers based on a silicon oxide backbone. These silica-based sol-gel materials provide the rigid and compact matrix into which different functional components, even from biological origin, can be incorporated. Both small organic moieties and polymeric/oligomeric species can be either chemically bonded to the monomer structure (generating the so-called organo-alkoxysilanes) and/or physically entrapped in the silicon oxide inorganic network to produce organic/inorganic hybrid network structures [11]. These materials combine the merits of inorganic glasses and organic molecules. They can be tailored to be transparent over a wide wavelength range and to have an adequate refractive index [12], which makes them very attractive for the fabrication of low-cost photonic components [13] such as waveguides [14], diffraction gratings [15] or microlenses [16]. The combination of hybrid polymeric materials with simple and inexpensive techniques of microfabrication, such as the well-known *soft lithography* [17] is envisaged to allow the development of components and analytical devices for viable commercial applications [18]. There are several *soft lithographic* techniques but most of them are based on the ubiquitous principle that makes use of an elastomeric stamp to replicate the patterns defined in a master fabricated by standard photolithography [19]. One of the major advantages of this technology is that it requires simple and non-expensive equipment; it is compatible with a variety of substrates regardless of their topography, thereby making this technology very attractive for simple large-scale microfabrication processes.

Since the pioneering work of Avnir and associates, who entrapped Rhodamine-6G into pure silica [20], a large number of molecules and biological species showing optical activity have been entrapped inside either an inorganic or a hybrid organic-inorganic network made by the sol-gel approach. A wide variety of material formulations showing different optical properties have been developed and excellent reviews showing their potential for the fabrication of photonic components and optical sensors have been published [13], [21–24]. However, few reported works deal with the patterning of these materials and none of them have shown their potential for the fabrication of absorbance micro-filters.

In this work we present the fabrication by a *soft lithography* approach of simple and low-cost absorbance filters based on a dye doped hybrid organic-inorganic xerogel polymer suitable to be monolithically integrated into a PhLoC. These filters show relatively sharp stopbands and almost zero passbands. The filtering capacity is a function of the nature of the dye and has a linear dependence with the filter width and the dye concentration. Their successful performance and potential to be easily integrated into disposable PhLoCs as well as in other microsystems is shown.

2. Experimental

2.1 Design

A 230-μm thick filter test structure was fabricated based on a previous work carried out in our lab [7]. Certain design modifications of the testing structure were introduced, while keeping the filter fabrication approach. That is a single continuous filter channel with different widths, which once filled with the polymer material, as described below, included different filtering sections with the same dye concentration but varying optical path (Fig. 1 (a)). One of the major advantages of such structure is that identical experimental conditions are applied in all filters included in the same testing structure. Then, more reliable comparative studies can be carried out. To improve reliability regarding the influence of the optical path length in the filtering capacity, sections widths were increased from four [7], to eight, i.e. –100, 250, 500, 1000, 1500, 2000, 2500 and 3000 μm. These widths define the propagating distance of the filters, resulting in the implementation of eight different filters in the same structure. Herein,

#168632 - $15.00 USD Received 15 May 2012; revised 6 Jul 2012; accepted 23 Jul 2012; published 1 Oct 2012

the filter channel included two microfluidic ports at both ends for adequate structure filling with the pre-polymerization solution. The entire channel is filled by capillary forces starting from the side with the largest width. In the former structure, the filling process made use of opens at both ends of the channel that appear at the edge of the mold. The new design included input and output holes on the surface of the mold thus avoiding the accumulation of residual material at both sides of the mold. These top holes also reduced the quantity of pre-polymerization solution needed to block the apertures (in order to prevent the emptying of the structure) due to their smaller size, circular shape and position. Xerogel materials tend to shrink when are synthesized due to the loss of volume caused by solvent evaporation. In this context, diamond-shaped widenings were designed at both sides of the filling channel that act as pre-polymerization solution reservoirs for re-filling of the filtering channel during the polymerization process and thus preventing the formation of air bags that could distort the resulting filter structures. These were not necessary in the previous PDMS-based approach because this material shows negligible shrinkage while curing [7]. The system is completed with self-alignment channels for positioning of the input and output optical fibers at both sides of every filter, together with microlenses at the end of every self-alignment channel for correcting the numerical aperture of the used fiber optics [25]. In the new design, these elements were implemented as components separated from the self-alignment channels in order to prevent possible damage or malfunction of the microlenses due to bad positioning of optical fibers.

2.2 Fabrication

The material synthesis and the fabrication of the test structure by soft lithography are the two main steps to develop the polymeric absorbance micro-filters.

2.2.1 Material synthesis

The pre-polymerization solution (*sol*) was prepared by mixing phenyltrimethoxysilane (PhTMOS) monomer (Sigma-Aldrich Química S.A., Spain) with dye aqueous solutions at pH 3 (adjusted with diluted HCl). Four different dye concentrations in the aqueous solution were used: 10, 50, 100 and 200μM.The silane: water molar ratio was 1:6. The selected dyes for this study were quinoline yellow (QY), phenol red (PR), methyl orange (MO) and crystal violet (CV) (all of them from Sigma-Aldrich Química S. A., Spain), whose absorbance bands show maximum absorbance values at 420, 515, 530 and 600 nm wavelengths, respectively. These dyes were selected to cover most of the visible spectrum. Except QY, these dyes are pH sensitive, showing different color for the acidic and the basic form; PR, yellow to red (pH, 6.8-8.0), MO, red to orange-yellow (pH 3.1-4.4), CV, yellow to blue (0.0-1.8).The mixture was gently stirred using a magnet until a homogeneous solution was achieved taking around 4h. At this point the resulting *sol* solution was ready for filling the test microstructure.

2.2.2 Fabrication of the test microstructure

The structure from which the eight micro-filters were obtained was fabricated by a soft lithographic approach. The master was developed using the SU-8 photocurable polymer in a one-step photolithographic process. SU-8 2025 (Microresist Technology GmbH, (Berlin, Germany)) was used to obtain a layer with a thickness of 230 μm by spin-coating [26]. PDMS pre-polymer solution (Sylgard 184 elastomer kit, Dow Corning Corp, (Midland, MI)) used for the replication of the master was made by mixing the silicon elastomer with the curing agent in a 10:1 ratio (v: v). Then, it was carefully poured over the SU-8 master. Once cured at 80°C for 20 minutes, the PDMS was peeled off the master with the aid of tweezers. The resulting PDMS test structures were irreversibly bonded to glass slides by a conventional oxygen plasma process [27]. The fluidic ports included in the test structures, as described above, were opened and the microstructure was filled with the *sol* solutions. Filling was achieved by capillary forces, thus avoiding the use of external pumps. The polymer was left to cure and

#168632 - $15.00 USD Received 15 May 2012; revised 6 Jul 2012; accepted 23 Jul 2012; published 1 Oct 2012

dry at room temperature for 4-5 days. The curing time could be reduced to 1 h by applying a temperature of 80 °C, without observing any alteration of the resulting material structure. The dye-doped xerogel structure was thus formed and the filters were ready to be tested. Figure 1(b) show a picture of polymeric micro-filters fabricated in the PDMS test structure using a xerogel polymer doped using a 200 μM CV solution.

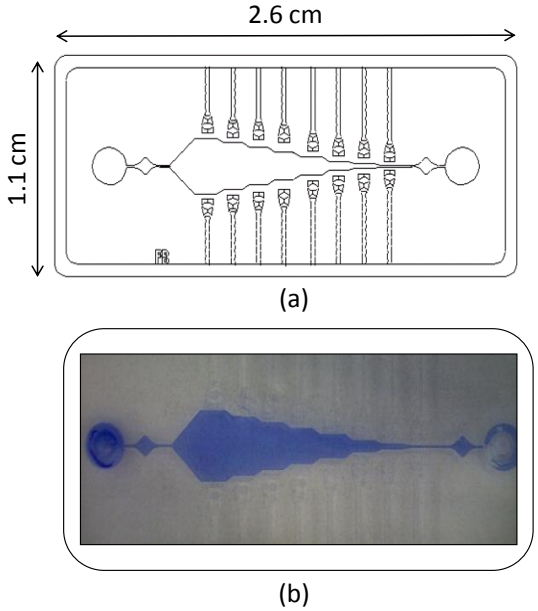

Fig. 1. (a) Design of the mask used for the fabrication of the testing microstructure (b) Crystal Violet doped xerogel micro-filters.

3. Material & structural characterization

In order to give some insight into the resulting doped polymer matrix, FT-Infrared Spectroscopy (Tensor 27 FT-IR spectrophotometer including a MKII Golden Gate Single Reflection ATR module, Bruker Corporation, Germany), ^{29}Si-Magnetic Nuclear Resonance (^{29}Si-NMR single-pulse (SP) solid state magic angle spinning nuclear magnetic resonance, Bruker Avance 400 spectrometer, Bruker Corporation, Germany) and Scanning Electron Microscopy (SEM) studies were carried out. Measurement of dye-doped and non-doped xerogel refractive indexes was kindly carried out by Metricon Corporation (NY,USA) using the Metricon Model 2010/M Prism Coupler equipment, which determines the refractive index from (m-line) layer modes [28]. The material transparency was also tested by collecting light passing through a drop-coated xerogel glass slide.Fig. 2, Fig. 3, Fig. 4, Fig. 5, Fig. 6, Fig. 7

The material is transparent over the entire visible spectrum and near infrared region (Fig. 8, appendix). ^{29}Si-NMR spectroscopy study provides information about the degree of condensation in the resulting polysiloxane matrix [29, 30]. The number of siloxane bonds that surround each silicon atom is determined from characteristic signals. Si atoms from PhTMOS can only form a maximum of three bonds and are responsible for T^n signals where n is the number of oxygen atoms bonded to silicon and forming siloxane bridges (Si-O-Si) with adjacent silicon atoms. These signals have been widely observed when analyzing xerogel materials with different compositions. Indeed, the ^{29}Si-NMR spectrum of the non-doped xerogel (Fig. 9, appendix) signals at –69.8 ppm and –79.5 ppm assigned to T^2 and T^3, respectively. The relative area of the T^3/T^2 signals in this material are 43/57, which indicates a high degree of condensation with 43% of Si atoms involved in three siloxane bonds. The spectrum of the dye-doped (CV) xerogel (Fig. 9) showed the same displacement for the two

#168632 - $15.00 USD Received 15 May 2012; revised 6 Jul 2012; accepted 23 Jul 2012; published 1 Oct 2012

signals but with different areas. The polycondensation of hydrolyzed PhTMOS seem to be slightly affected by the addition of the CV dye with 49% of Si atoms involved in three siloxane bonds resulting in a more cross-linked structure than the one of the non-doped material. This difference is likely to be related to the acid base nature of the dye, which nonetheless may have a positive influence in the avoidance of dye leaching from the polymer network. The FT-IR study (Fig. 10, appendix) revealed that the incorporation of the dye into the polymer matrix has a negligible effect on the polymeric structural properties. FTIR spectra for both non-doped and dye-doped material show the characteristic bands for the bending and stretching of the Si-O bond (in the zone of 1000 cm^{-1}) as well as characteristic bands ascribed to the phenyl ring (C = C, 1600 $cm^{-1}$and 1475 cm^{-1}, C-H, 3150-3050 cm^{-1}). If the inclusion of dyes had altered the polymeric process and thus the resulting xerogel composition this would have been reflected in the disappearance and/or formation of bands in the spectra.

SEM images were also recorded and showed a smooth and crack-free xerogel material that perfectly replicated the pattern on the PDMS stamp (Fig. 2). The refractive index of both the non-doped and dye-doped xerogel materials, measured at λ = 633 nm was 1.5663 ± 0.0001 (n = 6), which again corroborates the negligible effect of the doping process on the xerogel optical and structural properties.

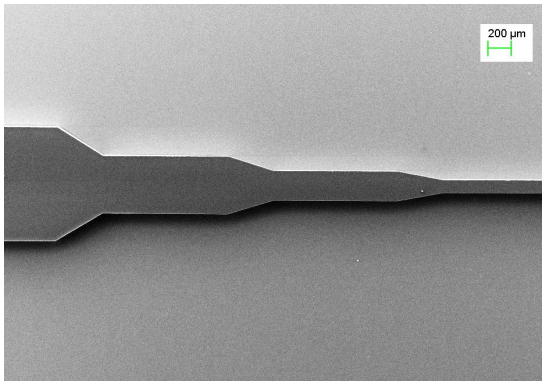

Fig. 2. SEM image of 100, 250, 500 and 1000 µm side xerogel microfilters fabricated in the same microstructure.

4. Spectral analysis

The setup for the analysis included a broadband halogen lamp as light source (HL-2000, Ocean Optics, Dunedin, FL, USA), two 230 µm diameter multimode optical fibers (Thorlabs Inc., Dachau, Germany) for coupling and collecting the light and a microspectrometer (QE 65000-FL, Ocean Optics, Dunedin, FL, USA). All filters were scanned in a wavelength region between 300 and 1000 nm with an integration time of 50 ms.The non-doped xerogel filter microstructure was fabricated and measured under the same experimental conditions and used as a reference.

Two of the most important parameters to characterize a filter are the rejections levels at the stopband (blocked wavelengths) and the transmission levels at the passband (allowed wavelengths) [2]. Figure 3 illustrates the transmittance values for the 200 µM dye-doped, 3000 µm wide filters. Minimum transmittance values at the stopband vary from −7 dB (for MO) to values below the dynamic range limit of our experimental setup (which was measured to be −26 dB) for CV (see Table 1). In the case of CV-based filters only an estimation of the transmittance can be provided. Here, by fitting the transmittance dependence with the filter width to an exponential decay function, the maximum transmittance values for the 2000, 2500 and 3000 µm-wide filters can be estimated to be −28.7, −30.7 and −31.9 dB, respectively. By comparing these values with the ones recorded in our previous work, where transmittance

#168632 - $15.00 USD Received 15 May 2012; revised 6 Jul 2012; accepted 23 Jul 2012; published 1 Oct 2012

values at the stopband were between −2 dB and −24 dB, a clear improvement was attained. They also outperformed those ones reported by Yamazaki *et. al* [8], who recorded transmittance values between −6 dB and −20 dB with dye-modified titanium oxide filters. In addition, they are of the same order of magnitude to those reported with dye doped photoresist based filters fabricated by Richard *et. al*. [9], which showed values from −5 dB to −32 dB. The state-of-the-art in integrated absorbance-based filters generally includes approaches with broad absorption bands that restrict their applicability to high-pass filters [6–9]. By contrast, this work reports almost zero passband values (Table 1) and relatively sharp stopbands (Fig. 3) recorded with all the fabricated xerogel polymeric absorbance microfilters. It should be noted that the nature of the dye determined the absorption capacity and the working wavelength, resulting in very different transmittance values for the same dye concentration and filter width. As previously discussed, the dyes selected in this work covered most of the visible spectrum. Nevertheless, other hydrosoluble dyes could also be incorporated inthe same polymeric material, as could be aniline blue (with a maximum absorption wavelength at 620 nm). Specific selection of the dye would basically depend on the required wavelength filtering. Figure 4 shows the recorded transmittance spectra of 300 µm-wide filters fabricated with the xerogel material doped with different concentrations of PR. The expected decrease in transmittance values at the stopband as the dye concentration increases is observed. Additionally, a secondary stopband, associated with the yellow acidic form of PR can be observed at short wavelengths (close to 450 nm). An almost zero passband value is also shown in Fig. 4, which means that the material exhibits a high transparency at wavelengths above 570 nm. The same study was carried out with those filters fabricated with the xerogel doped with QY, MO and CV and results are shown in Fig. 11 (appendix).Table 2

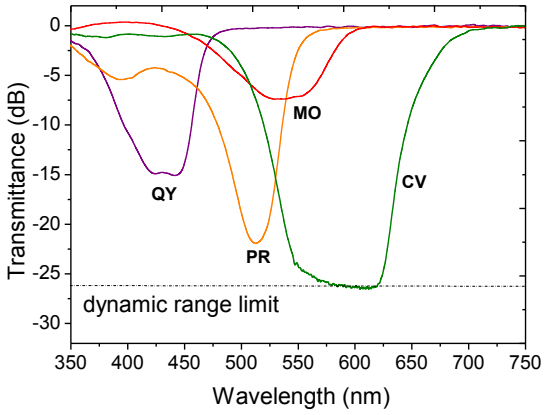

Fig. 3. Transmittance vs. wavelength for four different 200 µM dye-doped, 3000 µm wide filters.

The overall dimension of the filter is one of the most important premises from the miniaturization and integration point of view. It is clear that the longer the optical path, the higher the absorption but this goes against integration. This issue can be tackled by increasing the dye concentration for a fixed optical path. Figure 5 illustrates the transmittance values of PR-based filters at the stopband wavelength of 515 nm as a function of filter width and dye concentration. The result of the same study carried out with the QY, MO and CV based filters is shown in Fig. 12 (appendix). A linear trend when transmittance values were plotted against the filter width and dye concentration is observed in all cases as expected according to the Beer-Lambert law. For filters showing a width of 2000 µm and above, as well as for those

#168632 - $15.00 USD Received 15 May 2012; revised 6 Jul 2012; accepted 23 Jul 2012; published 1 Oct 2012

containing the highest dye concentration, saturation was reached in all cases. Most importantly, passband values still retain the value close to zero for all the tested filters (Tables 3-6, appendix). These results show that the dyes are homogeneously dispersed into the xerogel matrix without causing aggregates or phase separation, which may lead to scattering centers, and therefore decrease the transmittance in the passband region, as it was the case in our previous work with ink-doped PDMS [7].

Table 1. Stopband and passband transmittance values of the 3000 μm wide filters fabricated with the doped xerogel material (200 μM)

Dye	Stopband		Passband	
	λ [nm]	Transmittance [dB]	λ [nm]	Transmittance [dB]
Quinoline Yellow	420	–14.7	530	–0.2
Phenol Red	515	–21.8	575	–0.2
Methyl Orange	530	–7.4	650	–0.2
Crystal Violet	600	–31.9*	700	–0.5

*Theoretically estimated value.

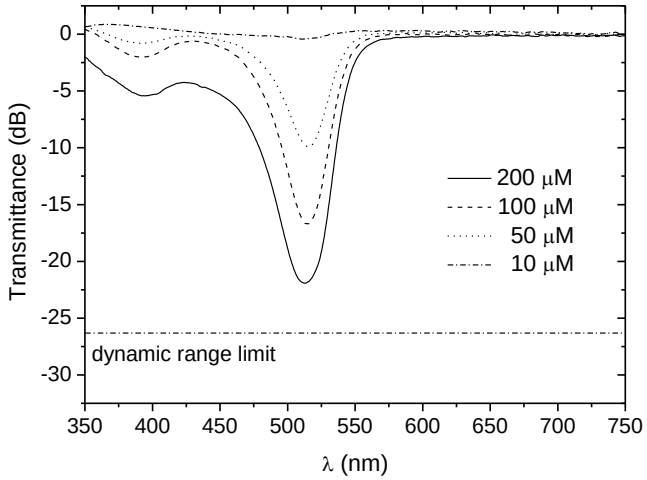

Fig. 4. Transmittance vs. wavelength for the 3000 μm widefilters fabricated with the xerogel polymer containing PRdyefor the four different concentrations tested.

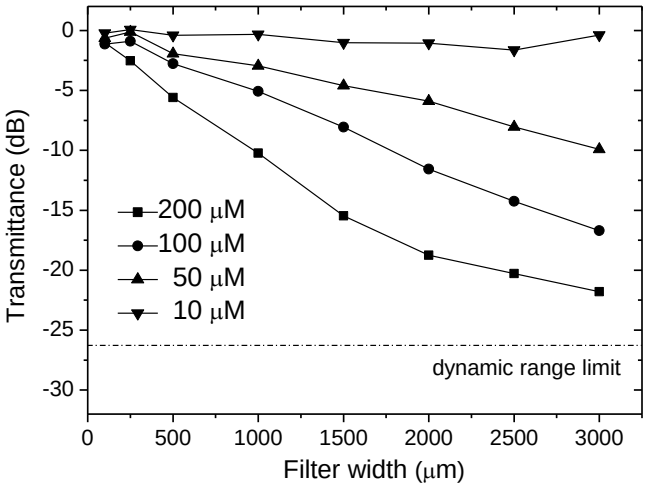

Fig. 5. Transmittance as a function of filter width for the PR doped polymeric filters.

#168632 - $15.00 USD Received 15 May 2012; revised 6 Jul 2012; accepted 23 Jul 2012; published 1 Oct 2012

5. Integration of the filters in a PhLoC

Once the viability of developing low-cost absorbance-based microfilters was shown, the following step involved their monolithic implementation in a PhLoC system. For this purpose, the microdevice presented in Fig. 6 was designed and then fabricated using the same soft-lithographic approach described above for the development of the filter test microstructures. Rhodamine B (ε = 106.000 $cm^{-1}M^{-1}$) was selected as a model target analyte to be measured in the PhLoC system. The reasons for selecting this target analyte are two-folded. Firstly, the absorption band can be used for calibrating the response of the PhLoC to analytes that have a specific absorption band but do not show photonic re-emission (as could be colorants or indicators) [31]. Secondly, the emission band can also be studied to validate the technological filtering approach presented in this work for measuring analytes with photonic re-emission (as could be quantum dots or fluorophores).The absorption and emission bands of Rhodamine B fluorophore are centered at 540 nm and 616 nm, respectively. Among the different filters fabricated and characterized the one that best fits for the measurement of this fluorophore is the PR-doped one, which, as shown in the previous section, shows a sharp stopband, from 450 nm to 540 nm (with maximum absorption at 515 nm) and an almost zero passband value outside this range. It was clearly shown that the wider the filter, the higher the stopband value. Nevertheless, keeping in mind that the aim of this work is to develop a filter suitable to be integrated in a PhLoC, a compromise between the overall dimensions of the filter and the filtering capability has to be reached. In our case, we selected a filter width of 800 μm fabricated with the xerogel material doped with the highest concentration of PR tested. It could be anticipated that this filter configuration would be suitable for our purposes considering the values of the stopband attained with a 1000 μm-wide filter (−10.2 dB@515 nm). Considering the previously shown Beer- Lambert behavior of all the filters tested, transmittance values of −8.2 dB at the stopband and almost zero at the passband were expected for this filter configuration. Two readout channels (for the alignment of the collection optical fiber) located at 90° and 180° from the input channel (injection optical fiber) were easily integrated in a single microdevice. However, with the aim of performing the test in the less-favorable conditions possible, only the most challenging configuration of 180° between injection and collection optical fibers was used. Eight different solutions of the Rhodamine B fluorophore prepared in dionized (DI) water in a concentration range from 25 μM to 500 μM were sequentially injected into the microfluidic channel (60 μm width). The set-up used is shown in Fig.S6. It included a 100 mW monochromatic green light (532 nm, Laser module NANO 250-532-100, Linos Photonics, Germany) as light source. The light was coupled into the system by a 230 μm in diameter multimode optical fiber (Thorlabs, Dachau, Germany) and collected by an identical one. The collection fiber was positioned in the self-alignment channel located after the PR filter (Fig. 13, appendix). Thus, light passed through the filter before reaching the spectrometer.

#168632 - $15.00 USD Received 15 May 2012; revised 6 Jul 2012; accepted 23 Jul 2012; published 1 Oct 2012

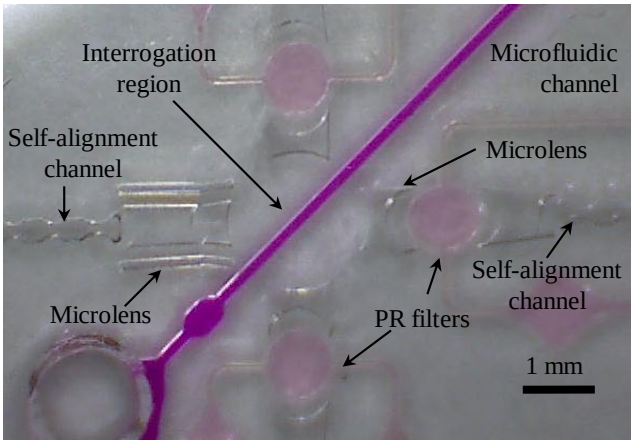

Fig. 6. Image of the fluorescence LOC with integrateddye-doped polymeric filters.

For comparative purposes, two identical systems were measured, the only difference being the presence of either a non-doped or a PR doped xerogel acting as a filter. For each dilution absorbance and fluorescence spectra were recorded. A the linear fit was carried out and the limit of detection (LOD) calculated following the IUPAC criteria, which states that the LOD is not the lowest detectable analyte concentration, but also depends on both the sensitivity and the accuracy of the linear fit, thus being determined as theleast concentration of analyte for which the signal exceeds by a factor of 3 the relative standard deviation of the background signal divided by the slope of the calibration curve [32].

Absorbance vs. Rhodamine B concentration shown in Fig. 7A shows the expected linear trend in accordance with the Beer-Lambert law at a wavelength of 540 nm. When compared the results recorded using identical PhLoC with and without the integrated filter (Table 2), it can be seen that the performance of the former has been significantly improved, with a three-fold increase in sensitivity while the LOD was reduced by 35%. This enhancement can be understood from the fact that the PR filters eliminates background light that causes random variations of the readout signal.

Fluorescence vs. Rhodamine B concentration was also studied, and the results are shown in Fig. 7B and Table 2. It can be seen how the integration of the PR filters is key to carry out fluorescence measurements in the system. When the filters were not included, the sensitivity (slope of the calibration curve) can be considered to be zero, and the LOD has a value higher than the concentration range measured, which basically means that it is not possible to determine the fluorescence. By contrast, when the PR-doped xerogel filter was included, a linear trend between Rhodamine B concentration and fluorescence measured at 616 nm was clearly obtained in a concentration range between 25 μM and 350 μM, the estimated limit of detection being 29 ± 1 μM. This value compares well with the ones reported by Yamakazi *et. al.* [8], who positioned 500 μm path-length cuvettes containing different concentrations of Rhodamine 6G on top of different absorbing layers. They reported LODs of 1.9 μM and 2.5 μM, similar to the one we obtained taking into account the difference in path lengths and the slightly higher extinction coefficient of Rhodamine 6G (ε = 116.000 $cm^{-1}M^{-1}$). When comparing these results with these previously reported, it can be seen that these xerogel-based absorbance filters outperform our previous ink-doped PDMS absorbance filters, while retaining the easy integration and the low cost issues [7]. Other contributions regarding optical filters for PhLoC applications can be highlighted, as could be Pais *et. al.* [33], who reported a 0.1 μM LOD measuring Rhodamine 6G in a disposable lab-on-chip including a cross polarization scheme, and Yao *et. al.* [34] who reported a 13-fold increase in sensitivity for a 300 μM Rhodamine 6G solution by implementing an interference filter in a microfluidic

#168632 - $15.00 USD Received 15 May 2012; revised 6 Jul 2012; accepted 23 Jul 2012; published 1 Oct 2012

device. Nevertheless, both approaches rely on either expensive technological steps and/or the alignment of several elements, which hampers the filter applicability in disposable

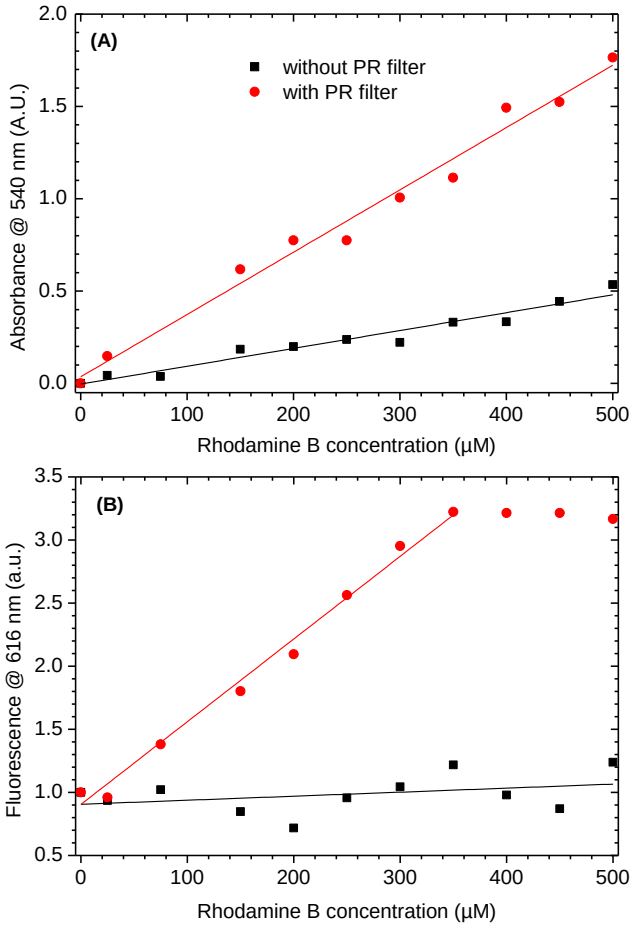

Fig. 7. a) Absorbance as a function of Rhodamine B concentration measured at 540 nm. b) Fluorescence emission as a function of Rhodamine B concentration measured at 616 nm. Fluorescence values were normalized considering fluorescence to have a unity value when the microchannel was filled with DI water.

Table 2. Linear fits, R^2 and LOD of the PhLoC with and without phenol red filter used during the rhodamine B calibration

	Linear fit	R^2	LOD (µM)
Abs_{540} without PR filter	$Abs_{540} = (9.7 \pm 0.7)x10^{-4}C-(3.4 \pm 0.1)\ x10^{-3}$	0.95	65 ± 4
Abs_{540} with PR filter	$Abs_{540} = (3.4 \pm 0.1)x10^{-3}C-(3 \pm 4)\ x10^{-2}$	0.98	42 ± 2
$Fluo_{616}$ without PR filter	$Fluo_{616} = (3 \pm 3)x10^{-4}C-(9.0 \pm 0.8)\ x10^{-1}$	0.03	763 ± 658
$Fluo_{616}$ with PR filter	$Fluo_{616} = (6.5 \pm 0.3)x10^{-4}C-(9.0 \pm 0.6)\ x10^{-1}$	0.99	29 ± 1

#168632 - $15.00 USD Received 15 May 2012; revised 6 Jul 2012; accepted 23 Jul 2012; published 1 Oct 2012

6. Conclusions

It has been demonstrated that low-cost absorption micro-filters could be easily fabricated using a dye-doped xerogel hybrid polymer material with a simple soft-lithographic approach.The presented tailor-made hybrid organic-inorganic polymeric material was compatible with several dyes, which enabled the development of filters covering a wide wavelength range of the visible spectrum. The fabricated micro-filters showed low transmittance values at the stopband, reaching the dynamic range limit of the spectrometer in some cases. Passband transmittance values are close to zero in all cases. Filtering capacity of these filters was consistent with the Beer-Lambert law in all cases and strongly depended on the nature of the dye. The successful integration of these polymeric absorbance micro-filters in a fluorescence based disposable photonic lab-on-a-chip was also demonstrated by carrying out calibration studies using Rhodamine B as model fluorophore target analyte and showing the greatly improved performance of the system compared with that one where no absorbance filter structure was implemented. Also, it is shown that this filtering approach outperforms other previously reported structures considering the attained stopband (as compared to existing high-pass absorbance filters) as well as the ease of their fabrication and integration in analytical microsystems.

7. Appendix

Non-doped xerogel (%) transmittance vs. wavelength. ^{29}Si-MNR and FT-IR spectra of doped and non-doped xerogel. Transmittance vs. wavelength for the 3000 μm wide quinoline yellow, methyl orange and crystal violet, loaded filters for all the concentrations. Transmittance vs. filter width for the four dyes in all the concentrations. Spectral properties of the different filters. Setup used to carry out the measurements with the integrated micro-filters.

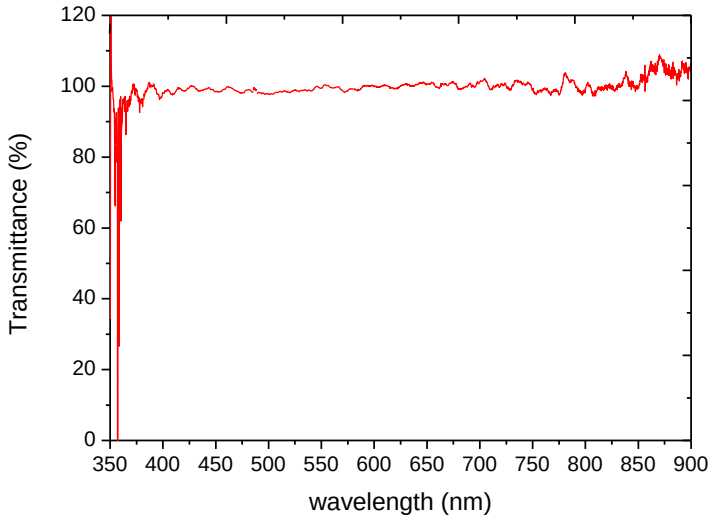

Fig. 8. Transparency of the non-doped xerogel material used in this work.

#168632 - $15.00 USD Received 15 May 2012; revised 6 Jul 2012; accepted 23 Jul 2012; published 1 Oct 2012

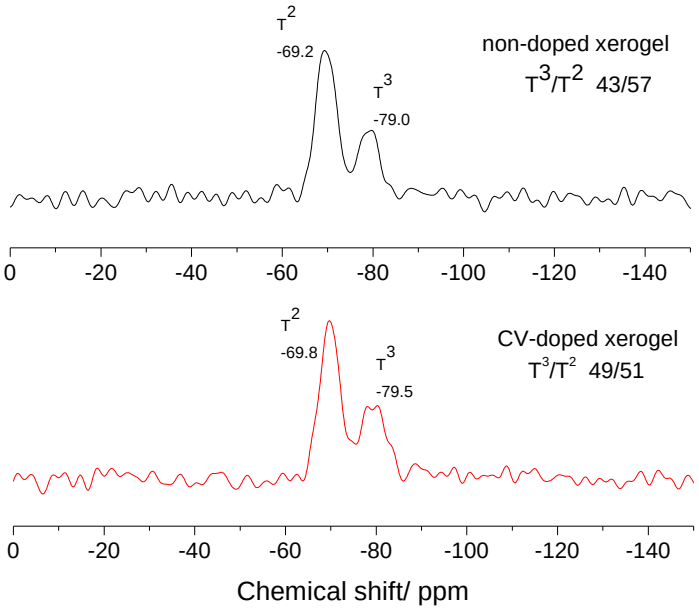

Fig. 9. ^{29}Si-NMR Spectra of the non-doped and crystal violet-doped hybrid polymer.

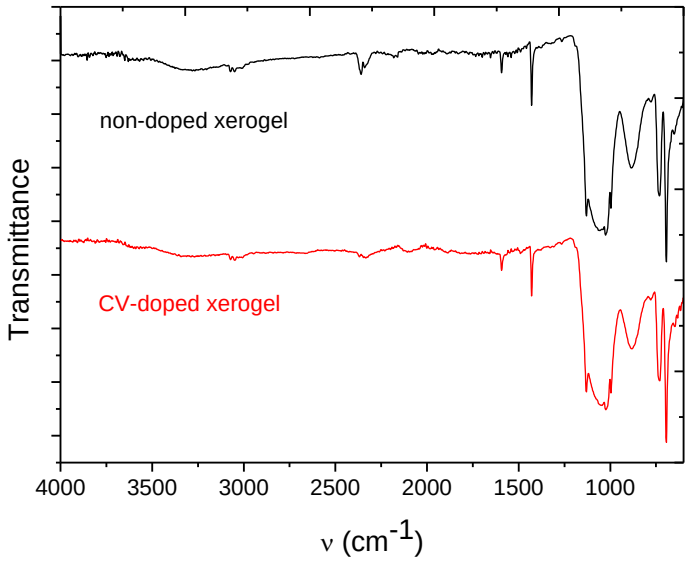

Fig. 10. FT-Infrared Spectroscopy spectra of the non-doped and dye-doped hybrid polymer.

#168632 - $15.00 USD Received 15 May 2012; revised 6 Jul 2012; accepted 23 Jul 2012; published 1 Oct 2012

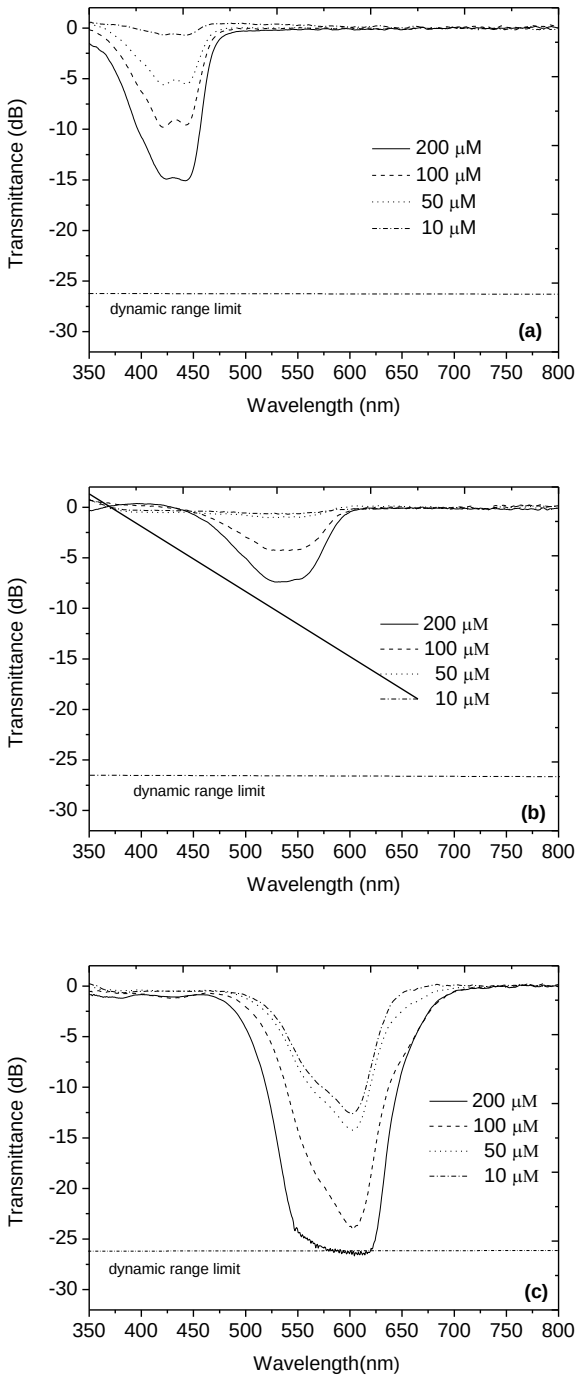

Fig. 11. (a) Transmittance vs. wavelength for the 3000 μm wide (a) quinoline yellow (b) methyl orange (c) crystal violet, doped filters for all the dye concentrations studied.

#168632 - $15.00 USD Received 15 May 2012; revised 6 Jul 2012; accepted 23 Jul 2012; published 1 Oct 2012

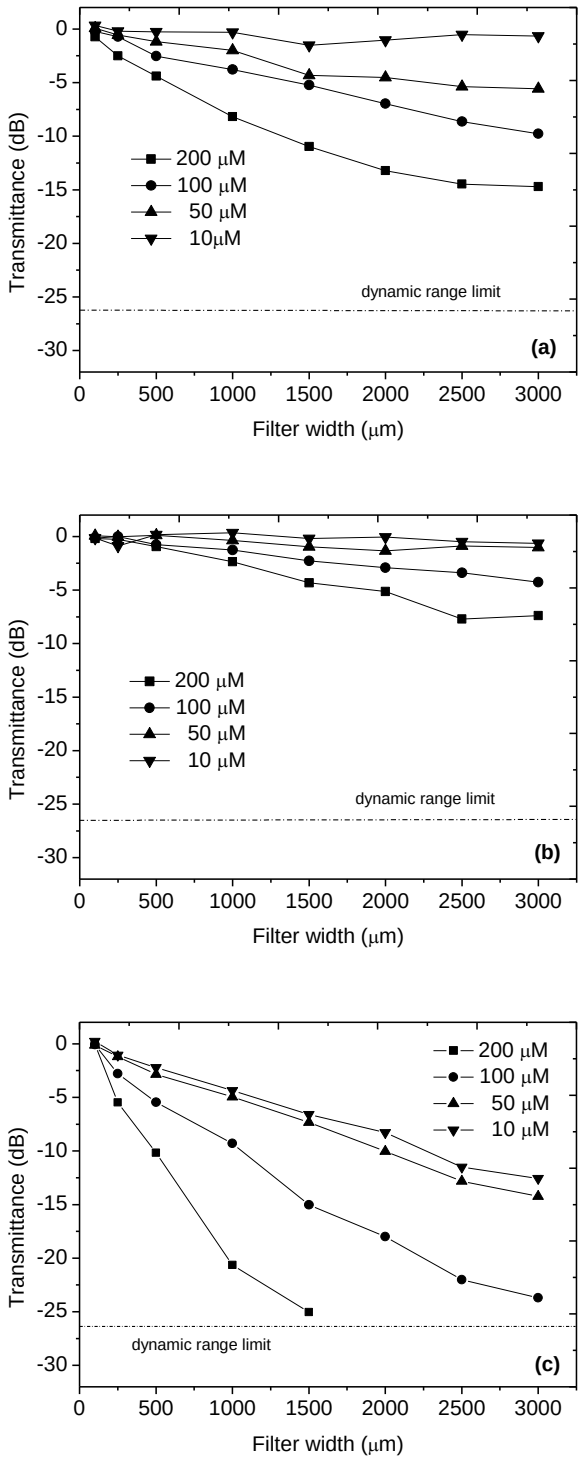

Fig. 12. Transmittance as a function of filter width for the (a) quinoline yellow (b) methyl orange (c) crystal violet, loaded filters for all the concentrations.

#168632 - $15.00 USD Received 15 May 2012; revised 6 Jul 2012; accepted 23 Jul 2012; published 1 Oct 2012

Table 3. Spectral properties of the quinoline yellow different filters. Positive values for transmittance are likely to be related to misalignment issues when measuring the reference test structure (non-doped xerogel filter structures).

		Stopband region		Passband region		
Dye concentration (μM)	Width [μm]	λ [nm]	Transmittance (T_s) [dB]	λ [nm]	Dye concentration (μM)	T_s - T_p
10	100		0.3	530	0.2	-
	250		–0.2		–0.1	–0.1
	500		–0.3		0.0	–0.3
	1000		–0.3		0.1	-
	1500		–1.5		–0.3	–1.2
	2000		–1.0		0.0	–1.0
	2500		–0.5		0.3	-
	3000		–0.7		0.4	-
50	100		0.1	530	0.1	-
	250		–0.6		–0.1	–0.5
	500		–1.2		–0.1	–1.1
	1000		–2.0		0.1	-
	1500		–4.3		–0.3	–4.0
	2000		–4.5		0.0	–4.5
	2500		–5.4		–0.2	–5.2
	3000		–5.6		0.0	–5.6
100	100		–0.2	530	0.1	-
	250		–0.7		0.1	-
	500		–2.5		–0.1	–2.4
	1000		–3.8		0.0	–3.8
	1500		–5.2		0.0	–5.2
	2000		–7.0		–0.1	–6.9
	2500		–8.6		–0.1	–8.5
	3000		–9.8		–0.1	–9.7
200	100		–0.7	530	0.2	-
	250		–2.5		0.0	–2.5
	500		–4.4		0.0	–4.4
	1000		–8.2		0.0	–8.2
	1500		–11.0		0.1	-
	2000		–13.2		0.0	–13.2
	2500		–14.4		0.0	–14.4
	3000		–14.7		–0.2	–14.5

Table 4. Continued from Table 3. Spectral properties of the phenol red different filters. Positive values for transmittance are likely to be related to misalignment issues when measuring the reference test structure (non-doped xerogel filter structures).

		Stopband region		Passband region		
Dye concentration (μM)	Thickness [μm]	λ [nm]	Transmittance (T_s) [dB]	λ [nm]	Transmittance (T_p) [dB]	T_s - T_p
10	100	515	–0.2	570	–0.2	0.0
	250		0.1		0.2	-
	500		–0.4		0.0	–0.4
	1000		–0.3		0.0	–0.3
	1500		–1.0		–0.1	–0.9
	2000		–1.1		0.0	–1.1
	2500		–1.6		–0.2	–1.4
	3000		–0.4		0.3	-
50	100	515	–0.6	570	–0.4	–0.2
	250		–0.1		0.2	-
	500		–1.9		–0.3	–1.6
	1000		–3.0		–0.1	–2.9
	1500		–4.6		0.0	–4.6

#168632 - $15.00 USD Received 15 May 2012; revised 6 Jul 2012; accepted 23 Jul 2012; published 1 Oct 2012

	2000		–5.9		0.1	-
	2500		–8.0		–0.2	–7.8
	3000		–9.9		0.1	-
100	100	515	–1.1	570	–0.4	–0.7
	250		–0.9		0.0	–0.9
	500		–2.7		–0.1	–2.6
	1000		–5.1		0.3	-
	1500		–8.1		0.1	-
	2000		–11.6		0.4	-
	2500		–14.2		–0.1	–14.1
	3000		–16.7		0.0	–16.7
200	100	515	–1.0	570	–0.3	–0.7
	250		–2.5		0.2	-
	500		–5.6		0.3	-
	1000		–10.2		0.2	-
	1500		–15.5		0.1	-
	2000		–18.7		0.1	-
	2500		–20.3		–0.1	–20.2
	3000		–21.8		–0.2	–21.6

Table 5. Continued from Table 4. Spectral properties of the methyl orange different filters. Positive values for transmittance are likely to be related to misalignment issues when measuring the reference test structure (non-doped xerogel filter structures).

		Stopband region		**Passband region**		
Dye concentration (μM)	Thickness [μm]	λ [nm]	Transmittance (T_s) [dB]	λ [nm]	Transmittance (T_p) [dB]	T_s - T_p
10	100	530	–0.1	650	–0.1	0.0
	250		0.9		0.1	-
	500		0.2		0.1	-
	1000		0.3		0.3	-
	1500		–0.2		–0.1	–0.1
	2000		0.0		0.1	-
	2500		–0.5		–0.1	–0.4
	3000		–0.6		–0.1	–0.5
50	100	530	0.1	650	0.0	-
	250		0.0		0.0	0.0
	500		0.1		0.0	-
	1000		–0.4		0.0	–0.4
	1500		–1.0		–0.1	–0.9
	2000		–1.3		–0.1	–1.2
	2500		–1.0		0.1	-
	3000		–1.0		0.1	-
100	100	530	–0.1	650	0.0	–0.1
	250		0.0		0.1	-
	500		–0.7		–0.2	–0.5
	1000		–1.2		0.1	-
	1500		–2.3		–0.1	–2.2
	2000		–2.9		0.0	–2.9
	2500		–3.4		0.0	–3.4
	3000		–4.3		0.0	–4.3
200	100	530	–0.2	650	–0.2	0.0
	250		–0.3		0.0	–0.3
	500		–0.9		0.1	-
	1000		–2.3		0.2	-
	1500		–4.3		–0.1	–4.2
	2000		–5.1		0.3	-
	2500		–7.7		–0.2	–7.5
	3000		–7.4		–0.1	–7.3

#168632 - $15.00 USD Received 15 May 2012; revised 6 Jul 2012; accepted 23 Jul 2012; published 1 Oct 2012

Table 6. Continued from Table 5. Spectral properties of the crystal violet different filters. Positive values for transmittance are likely to be related to misalignment issues when measuring the reference test structure (non-doped xerogel filter structures).

		Stopband region		**Passband region**		
Dye concentration (μM)	Thickness [μm]	λ [nm]	Transmittance (T_s) [dB]	λ [nm]	Transmittance (T_p) [dB]	T_s - T_p
10	100	600	–0.5	700	0.0	–0.5
	250		–1.0		0.0	–1.0
	500		–2.2		0.0	–2.2
	1000		–4.4		0.1	-
	1500		–6.6		0.0	–6.6
	2000		–8.3		–0.1	–8.2
	2500		–11.5		0.2	-
	3000		–12.6		0.1	-
50	100	600	–0.9	700	–0.1	–0.8
	250		–1.2		0.1	-
	500		–2.8		–0.2	–2.6
	1000		–5.0		0.2	-
	1500		–7.3		0.1	-
	2000		–10.0		–0.1	–9.9
	2500		–12.8		0.4	-
	3000		–14.2		–0.2	–14.4
100	100	600	–1.5	700	0.0	–1.5
	250		–2.8		0.0	–2.8
	500		–5.5		–0.1	–5.4
	1000		–9.3		0.1	-
	1500		–15.0		–0.3	–14.7
	2000		–18.0		–0.3	–17.7
	2500		–22.0		0.5	-
	3000		–23.7		–0.6	–23.1
200	100	600	–2.5	700	–0.1	–2.4
	250		–5.5		0.1	-
	500		–10.2		0.0	–10.2
	1000		–20.6		0.2	-
	1500		–25.0		–0.2	–24.8
	2000		out of range (- 28.7)[#]		–0.6	-
	2500		out of range (–30.7)[#]		0.9	-
	3000		out of range (–31.9)[#]		–0.5	-

[#]Estimated theoretical values.

#168632 - $15.00 USD Received 15 May 2012; revised 6 Jul 2012; accepted 23 Jul 2012; published 1 Oct 2012

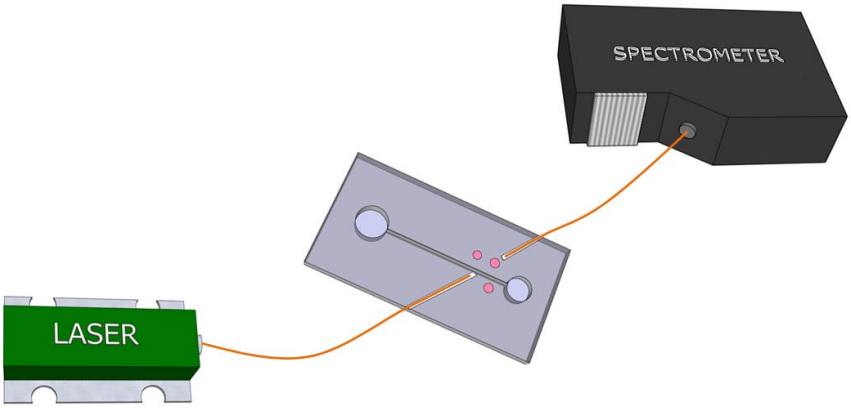

Fig. 13. Setup used to carry out the measurements of Rhodamine B target analyte in the PhLoC where the phenol-red based filters were implemented. It comprises a laser working at a2-5wavelength 532 nm, two multimode optical fibers and a spectrometer.

Acknowledgments

The research leading to these results has received funding from the European Research Council under the European Community's Seventh Framework Programme (FP7/2007-2013) / ERC grant agreement n° 209243 and from project ref. TEC2010-17274 (Spanish ministry of Economy and Competitivity). The authors would like to thank Dr. Manuel Gutiérrez-Capitán, from IMB-CNM (CSIC) and Dr. Magarita Darder from ICMM (CSIC), for their assistance with the FT-IR and the 29Si-NMR spectroscopic analysis, respectively.